IEEE Access
Multidisciplinary | Rapid Review | Open Access Journal

Received August 12, 2020, accepted August 25, 2020, date of publication August 31, 2020, date of current version September 14, 2020.

*Digital Object Identifier 10.1109/ACCESS.2020.3020266*

# Fast and Accurate Desnowing Algorithm for LiDAR Point Clouds

**JI-IL PARK[1], (Student Member, IEEE), JIHYUK PARK[2], (Member, IEEE), AND KYUNG-SOO KIM[1], (Member, IEEE)**

[1]Department of Mechanical Engineering, Korea Advanced Institute of Science and Technology, Daejeon 34141, South Korea
[2]Department of Automotive Engineering, College of Mechanical and IT Engineering, Yeungnam University, Gyeongsan 38541, South Korea

Corresponding authors: Jihyuk Park (jihpark@yu.ac.kr) and Kyung-Soo Kim (kyungsookim@kaist.ac.kr)

This research was financially supported by the Institute of Civil Military Technology Cooperation funded by the Defense Acquisition Program Administration and Ministry of Trade, Industry and Energy of Korean government under grant No. UM19303RD3.

**ABSTRACT** LiDAR sensors have the advantage of being able to generate high-resolution imaging quickly during both day and night; however, their performance is severely limited in adverse weather conditions such as snow, rain, and dense fog. Consequently, many researchers are actively working to overcome these limitations by applying sensor fusion with radar and optical cameras to LiDAR. While studies on the denoising of point clouds acquired by LiDAR in adverse weather have been conducted recently, the results are still insufficient for application to autonomous vehicles because of speed and accuracy performance limitations. Therefore, we propose a new intensity-based filter that differs from the existing distance-based filter, which limits the speed. The proposed method showed overwhelming performance advantages in terms of both speed and accuracy by removing only snow particles while leaving important environmental features. The intensity criteria for snow removal were derived based on an analysis of the properties of laser light and snow particles.

**INDEX TERMS** Snow noise removal, desnowing, autonomous vehicle, LiDAR point cloud filtering.

## I. INTRODUCTION

LiDAR sensors are used in autonomous vehicles primarily to complement the camera and radar. Therefore, most companies developing autonomous vehicles use LiDAR in conjunction with radar and cameras. However, some studies are based only on cameras and radars and omit LiDAR because of its poor performance under harsh weather conditions and high costs relative to other sensors. Recently, because the price of LiDAR sensors has been dropping, the cost problem has been solved to some extent; however, the problem of LiDAR's vulnerability to environmental changes still exists.

For these reasons, many researchers still actively conduct research using radar and camera combinations or perform sensor fusion of two sensors to implement autonomous driving in adverse weather conditions. Most of these studies are based on using deep learning algorithms or outlier filters to remove environmental noise such as snow or rain from images. Considering that LiDAR is clearly suceptible to adverse weather conditions, it is not surprising that very little research has been published on methods to desnow LiDAR point clouds [1]. Fortunately, as the LiDAR technology continues to develop and becomes affordable, interest in using LiDAR sensors in autonomous driving applications is increasing, and research to address the shortcomings of LiDAR is also becoming more active [2]–[6]. Recently, research on snow removal has been carried out by applying deep learning [7] or improving an existing filter [8], [9]. These studies significantly improved the accuracy and speed of snow removal. In particular, the snow-removal accuracy has been noticeably improved, but the snow-removal speed is still limited, which means that the currently developed snow removal filters are unsuitable for applications in autonomous vehicles.

Therefore, in this study, we propose a new snow removal filter that achieves speed and accuracy levels applicable to real-time autonomous driving. Two types of noise filters currently exist: a distance-based noise removal algorithm and a deep learning-based noise removal algorithm. In contrast, our proposed noise removal algorithm is based on intensity, which constitutes a new approach that is completely different from the previous two approaches. Although this approach represents a new challenge that has not been previously attempted, the proposed filter achieves surprisingly faster and more accurate performance than the existing filters.

The remainder of this article is organized as follows. In Section II, the methods for existing point cloud filters are analyzed. Our proposed filter and an explanation of how it

The associate editor coordinating the review of this manuscript and approving it for publication was Ikramullah Lali.

works are introduced in Sections III, IV and V, respectively. Finally, Section VI concludes the paper.

## II. EXISTING NOISE FILTERS FOR LiDAR POINT CLOUDS

### A. CONVENTIONAL NOISE FILTERS

Conventional noise filtering methods involve radius outlier removal (ROR), statistical outlier removal (SOR), and voxel grid (VG) filters [10]–[12]. The outlier removal filters can be applied to LiDAR point clouds; however, when used as noise filters for 3D LiDAR point clouds, they have some limitations in terms of speed and accuracy. Brief descriptions of the various filters are presented below.

#### 1) ROR FILTER

The ROR filter works on a simple technique: it computes the mean distance of each point to its neighbors within a certain search radius by using a k-d tree data structure. When the number of neighbors within a specified radius is below a given threshold, that point is removed. Thus, the performance of this filter depends on the specified radius and the minimum point threshold. It has the advantage of easy implementation but is difficult to apply to 3D LiDAR point cloud filters because it searches for neighbors within a fixed radius. Specifically, the distance between LiDAR points increases as the detection range distance increases due to the vertical and horizontal resolution of LiDAR. Thus, points located at relatively long distances are more likely to be removed as outliers due to their spacing.

#### 2) SOR FILTER

The SOR filter is similar to the ROR filter, but it does not use a fixed radius or a minimum point threshold to determine the neighbors. Instead, it computes the mean distance of each point to its neighboring points to considering the k-nearest neighbors. When those points are greater than the sum of the mean distance and the standard deviation, they are rejected. The performance of this filter depends on the number of nearest points, k, and the number of times the standard deviation is calculated. The problem with the SOR filter is that its filtering speed is slow because finding neighbors carries a high computational cost. Moreover, the greater the distance is, the higher the probability of a point being removed as an outlier (similar to the ROR filter).

#### 3) VOXEL GRID FILTER

The VG filter differs from the ROR and SOR filters in that it does not remove outliers based on the distance between points but rather downsamples the number of points. All points inside each voxel's predefined 3D box in 3D space are downsampled to an approximated voxel center point. This filter is sometimes considered to be a noise filter because the noise disappears. However, all the points are downsampled —not just the noise; therefore, this filter is only regarded as a downsampling filter, not a noise filter, because it removes not only outliers but also inliers based on the geometric information acquired during filtering.

### B. STATE-OF-THE-ART FILTERS

Recently, new noise filters for 3D point clouds have been proposed by improving an existing filter or applying deep learning. These studies achieve faster noise filtering speeds and higher accuracy compared to the existing conventional filters. First, we introduce the deep learning-based algorithms and then introduce methods for improving the existing filters.

#### 1) WeatherNet

WeatherNet is recently introduced denoising algorithm based on LiLaNet that is representative of approaches using convolutional neural networks. It performs pointwise, multiclass semantic labeling of semidense LiDAR data. WeatherNet can be optimized for denoising purposes by reducing the depth, inserting a dropout layer and adding a dilated convolution to the base block of the network. While WeatherNet achieves better performance than RangeNet and DROR [7], it is somewhat inappropriate to compare DROR to WeatherNet in dense fog situations because DROR was developed expressly for desnowing purposes. In dense fog situations, the performance of DROR deteriorates because of the differences in sparsity between snow and fog.

#### 2) FCSOR FILTER

The fast cluster statistical outlier removal (FCSOR) filter is an extension of the SOR filter [8]. This method consists of a voxel-subsampling step and an FCSOR step, and it reduces the computational complexity and running time by reducing the number of clusters and performing computations partially in parallel. However, it still does not achieve the performance levels required for snow removal because it focuses only on improving the speed by combining existing filters. Thus, it cannot be regarded as a suitable snow removal filter for 3D point clouds.

#### 3) DROR FILTER

A dynamic radius outlier removal (DROR) filter was developed to address the limitations of the ROR and SOR filters, which are based on a fixed radius and fixed numbers of neighboring points [9]. This enhanced filter reduces distant point losses by changing the search radius for neighboring points as the distance to the measured point increases. Consequently, it improves the accuracy by more than 90 % on point clouds acquired while driving in falling snow, and it is the most effective filter for removing snow without also removing other environmental features.

Similar to the filter proposed here, the DROR filter substantially outperforms the existing filters in terms of accuracy; consequently, it is highly suitable as a snow removal filter for 3D LiDAR point clouds. However, despite its good performance, DROR still has limitations that prevent it from being applied in real-time autonomous vehicles, such as its slow snow-filtering speed. This filter also has high computational costs because it is based on distance-based filters such as the ROR and SOR filters. The results of the various filters are reported in Section V.

## III. THE PROPOSED LIOR FILTER

### A. INTENSITY-BASED FILTERS

The proposed filter is a low-intensity outlier removal (LIOR) filter. As its name suggests, this filter eliminates snow by deleting points with intensity values below a specified intensity threshold. The idea behind the LIOR filter stems from the fact that the intensity of snow particles is lower than the intensities of other points at the same distance. LIOR differs from the existing SOR, ROR, and DROR filters in that it does not remove noise based on the distance between points. To date, many studies have performed classification or segmentation using LiDAR intensity values [13], [14], but to the best of our knowledge, this is the first attempt to remove noise based on intensity values.

Examination of the intensity values in a LiDAR point cloud acquired on a snowy day clearly reveals the intensity differences between snow and objects. Thus, we could confirm that snow particles have a very low intensity value compared to other nearby non-snow points, as shown in Figs. 1 and 2. The reason for applying the intensity value range from 0 to 1,000 is to visually distinguish snow from objects. When the intensity range is applied from 0 to 5,000 (which is the actual measured range), it is difficult to distinguish snow from objects, as most points are represented by a color close to red. This is because the intensity value of most points measured outdoors is lower than 1,000.

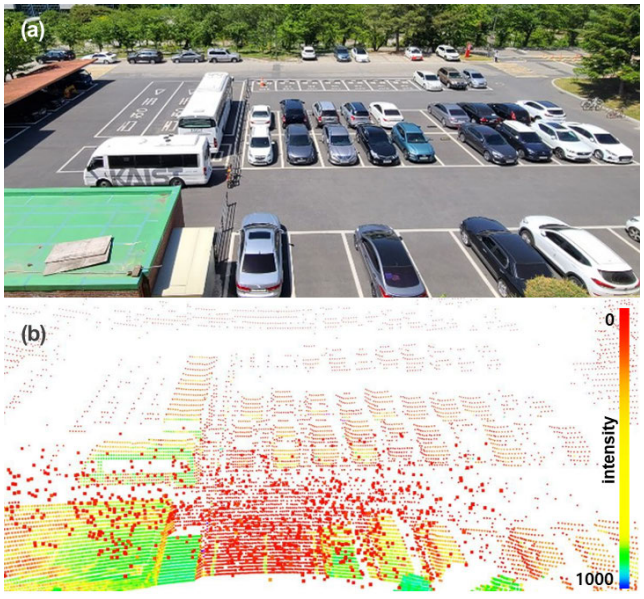


**FIGURE 1.** Parking lot image and point cloud. (a) Image taken on a clear day. (b) Point cloud acquired on a snowy day.

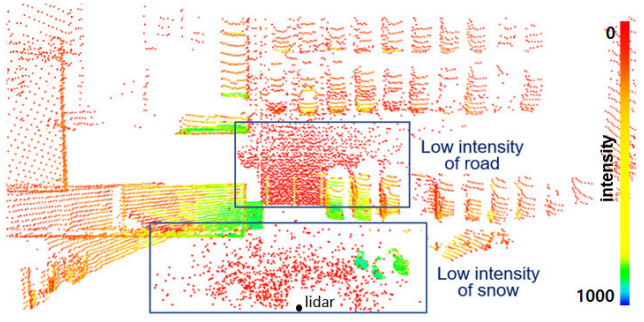


**FIGURE 2.** Point cloud acquired from a parking lot (plan view).

Fig. 2 shows that the intensity of the snow particles around the LiDAR and road surface have low values. Both the snow particles and the road surface have low intensities; however, the point spacing of the snow particles is sparse, while the point cloud density on the road surface is high.

### B. PRELIMINARIES

To design the LIOR filter, it is first necessary to select an intensity threshold to distinguish snow particles from ordinary objects. To this end, we first calculate the intensity curve of the OS-1 LiDAR used in the experiment. Given the intensity curve, the intensity values of the returned LiDAR light can be estimated at each distance. A snow removal threshold (covered in section IV) can then be determined based on the distance intensity values.

The intensity curve shown in (1) [15] reveals that the actual intensity value depends on the angle of incidence and object surface reflectivity [15]–[17]. The variables $I_{ref}$, $D_{ref}$, $D_c$, $I_c$, $\alpha$ and $R_s$ denote a reference intensity value, a reference point distance, a measurement distance, an intensity value corresponding to the measurement distance, the angle of incidence of the LiDAR light on the snow particle, and the object reflectance, respectively:

$$I_c = I_{ref} \cdot \frac{{D_{ref}}^2}{{D_c}^2} \cdot cos(\alpha). \tag{1}$$

To obtain the intensity curve corresponding to the LiDAR, the distance and intensity of the reference point were measured with the OS-1 LiDAR. First, as a reference point for deriving the intensity curve of the OS-1 LiDAR, an attempt was made to select a short distance point within 5 m, but the actual measurement result shows that the intensity deviation of the points located within 5 m are large, so the point located at 5.5 m showing a constant intensity value was selected as a reference point. For this reason, the point with an intensity value of 4,180, 5.5 m from the LiDAR, was selected as the reference value.

Additionally, to determine how the actual intensity changes with distance, it is assumed that the incident angle is 90 ° and the reflectance is 100 %. By applying these incident angles, the reflectance and reference point values are determined in (1), the intensity curve of OS-1 LiDAR is summarized in (2), and the final result of (2) is shown in Fig. 3. The intensity curve was cropped from 0 to 5,000, considering the maximum intensity value of OS-1 LiDAR.

$$I_c = 4,180 \cdot \frac{5.5^2}{{D_c}^2} = \frac{126,445}{{D_c}^2}. \tag{2}$$

## IV. PRINCIPLE OF LIOR

As explained in Section III, the principle underlying the LIOR filter involves removing the points with intensity values lower than a snow intensity threshold as outliers. In practice,

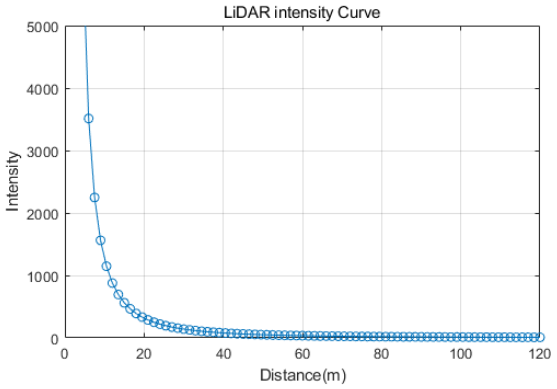


**FIGURE 3.** Intensity curve of OS-1 LiDAR.

filtering snow by applying this algorithm removes all snow particles in real time. However, the intensity values of close objects can be as low as that of snow particles depending on the differences in reflectance according to the material and color of the object's surface.

As shown in Fig. 4, even though cars are located immediately in front of the LiDAR sensor (within 3 m), some important points are lost when snow filtering is applied because of the low intensity values of some vehicle materials. To solve this problem, we developed a method to save the important points while omitting snow particles among the points classified as outliers that would otherwise be removed due to their low intensity values. In summary, this constitutes step 2, which reclassifies the non-snow outlier points removed in step 1 to inliers.

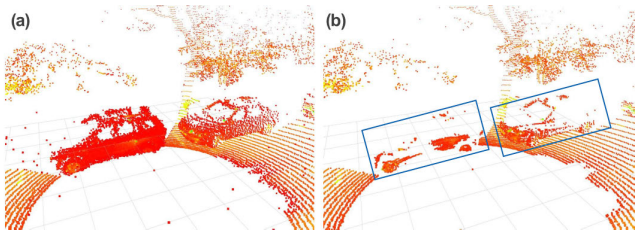


**FIGURE 4.** The results for the simple removal of points below the snow threshold intensity. The snow particles are completely removed. However, some points in the bounding boxes are also removed, even though they are not snow particles.

### A. LIOR FILTER DESCRIPTION

The LIOR filter consists of two steps. The first step identifies all points with an intensity below the threshold snow intensity value. The second step selects non-snow points that carry important environmental information from the outliers identified in step 1 and reclassifies them as inliers. To briefly describe the principle of the filter applied in step 2, when more than a certain number of neighbors exist within a specified radius among the outliers, the point is saved as an inlier.

The radius inlier saving (RIS) filter originated from the idea that the density of neighboring points located around snow particles is sparse, whereas the points classified as outliers, but not snow, have a much higher density of neighboring points, as shown in Fig. 4. The overall flow of the LIOR filter is described in the pseudocode in Algorithm 1, while a visual explanation of the RIS filter applied in step 2 is shown in Fig. 5.

**Algorithm 1** Pseudocode of LIOR

**for** $p \in P$ **do**
  computer the distance of the point $d_p$
  `// Determine the intensity threshold`
  **if** $d_p < d_s$ (71.235m) **then**
    $I_{thr} \leftarrow$ red line in Fig. 9
  **else**
    $I_{thr} \leftarrow 0$ ($\because$ no-snow area)
  **end if**
  `// Step 1: remove the snow points`
  **if** $I_p > I_{thr}$ **then**
    point $p$ classified as inlier $p_{in}$
  **else**
    point $p$ classified as outlier $p_{out}$
  `// Step 2: apply the RIS filter`
    count the number of neighbors $n_p$
    **if** $n_p > n_{thr}$ **then**
      outlier $p_{out}$ reclassified as inlier $p_{in}$
    **end if**
  **end if**
**end for**

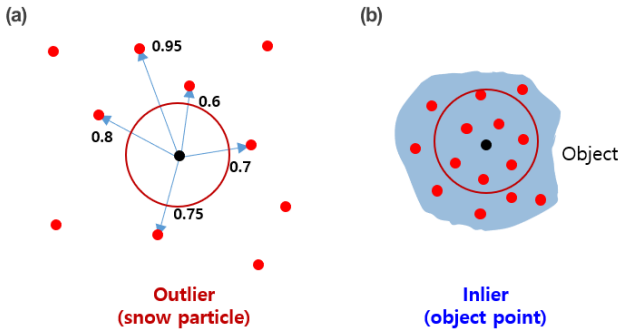


**FIGURE 5.** The RIS filter concept (specified points: 3, search radius: 0.5): (a) is a case that remained an outlier, and (b) is a case that was saved as an inlier.

### B. SNOW REMOVAL THRESHOLD

The key goal in this study is to find an appropriate snow removal threshold, which acts as the criterion for filtering snow. To derive the snow removal threshold, some basic knowledge of snow and light is required. First, because the intensity of light depends on the size, shape, and reflectance of snow particles, prior studies were conducted on the characteristics of snow.

Snow particle size was determined based on snow sizes collected in the Yeongdong region, the snowiest region in South Korea. Between 2017 and 2018, the maximum radius of snow particles was approximately 2.8 mm [20]. Thus, we can infer that the maximum size of a snow particle is

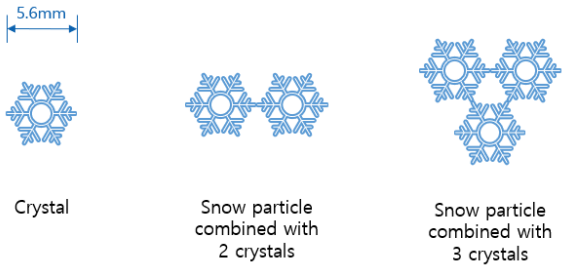


**FIGURE 6.** Maximum size of snow particles: The maximum size of a snow particle is 1.12 cm (considering up to three aggregated crystals).

5.6 mm. However, because this value corresponds to the size of individual snow crystals, it is difficult to regard it as representative of the actual size of all snow particles. Considering that snow crystals often aggregate in groups of two or three (a triangular shape) to become snow particles, the adopted maximum size for a snow particle was 1.12 cm.

After determining the size range for snow particles, the area ratio of the beam area to the snow area at the reference distance must be calculated. As shown in Fig. 7, at each distance, the intensity decreases in proportion to the square of the distance by the inverse square law. Here, because the area of a snow particle is smaller than the size of the beam, the exact amount of intensity impacting the snow particle can be calculated by considering the area ratio at the reference distance.

The angle of incidence when the light of LiDAR hit the snow particle was calculated under the assumption that all snow particles are spherical. That is, it was calculated in the same way as the method used to obtain the average angle of incidence when sunlight impacts the earth. As a result, the angle of incidence $\alpha$ is 45°.

The reflectance of snow particles was calculated by considering the 865-nm wavelength of OS-1 LiDAR [18], [19] and a snow particle size of 1.12 cm and is based on prior research results [20]. The reflectance was calculated based on experimental results showing that the reflectance decreases as the size of the snow particle increases. The reflectance corresponding to a snow particle diameter of 1.12 cm was 0.158. Based on an analysis of the characteristics of snow and OS-1 LiDAR, the following snow intensity threshold was ultimately obtained. The variables $I_{th}$, $AR$, and $R_s$ represent the snow intensity threshold, area ratio, and snow reflectance, respectively:

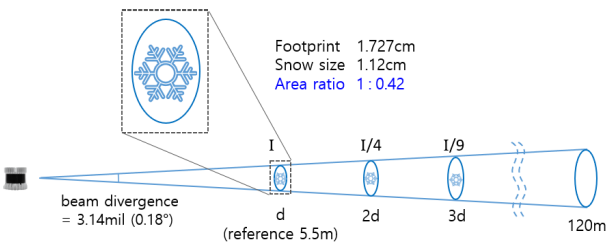


**FIGURE 7.** Area ratio of beam area to snow area.

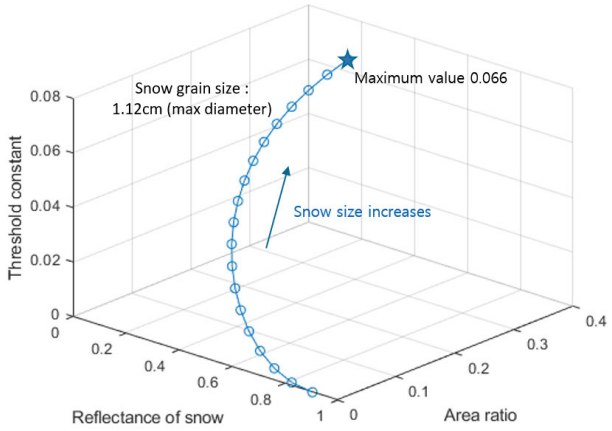


**FIGURE 8.** Changes in the intensity threshold constant according to snow particle size.

$$I_{th} = I_c \cdot AR \cdot cos(\alpha) \cdot R_s = 0.0469 I_c. \tag{3}$$

One important aspect is that as the snow particle size increases, the area ratio increases, while the reflectivity decreases; the intensity threshold constant is determined by multiplying these two parameters. Therefore, it is necessary to determine when the threshold constant multiplied by these two parameters reaches the maximum value.

As shown in Fig. 8, the two parameters have a trade-off relationship, but the threshold constant, which is the product of the two parameters, increases as the size of the snow particle increases. This means that the snow threshold constant is largest when the snow particle size reaches the maximum. Therefore, when the largest constant value is applied to the LIOR filter, all the snow particles below the maximum size will also be filtered.

The result of the snow intensity threshold is shown in Fig. 9. The blue line is the normal intensity curve ($I_c$) of LiDAR light, while the red line is the snow intensity threshold ($i_{th}$), which is the criterion for filtering snow. Consequently, the points under the red line represent the point cloud with the snow removed.

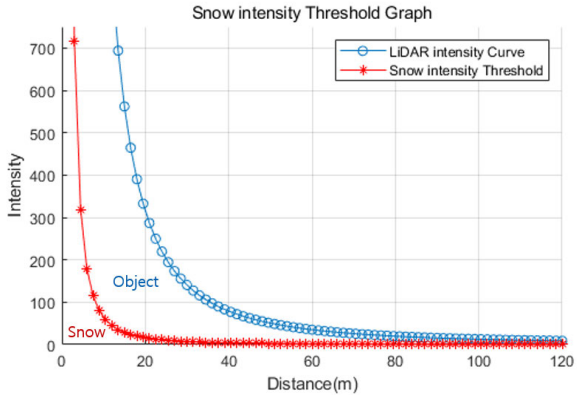


**FIGURE 9.** Snow intensity threshold graph.

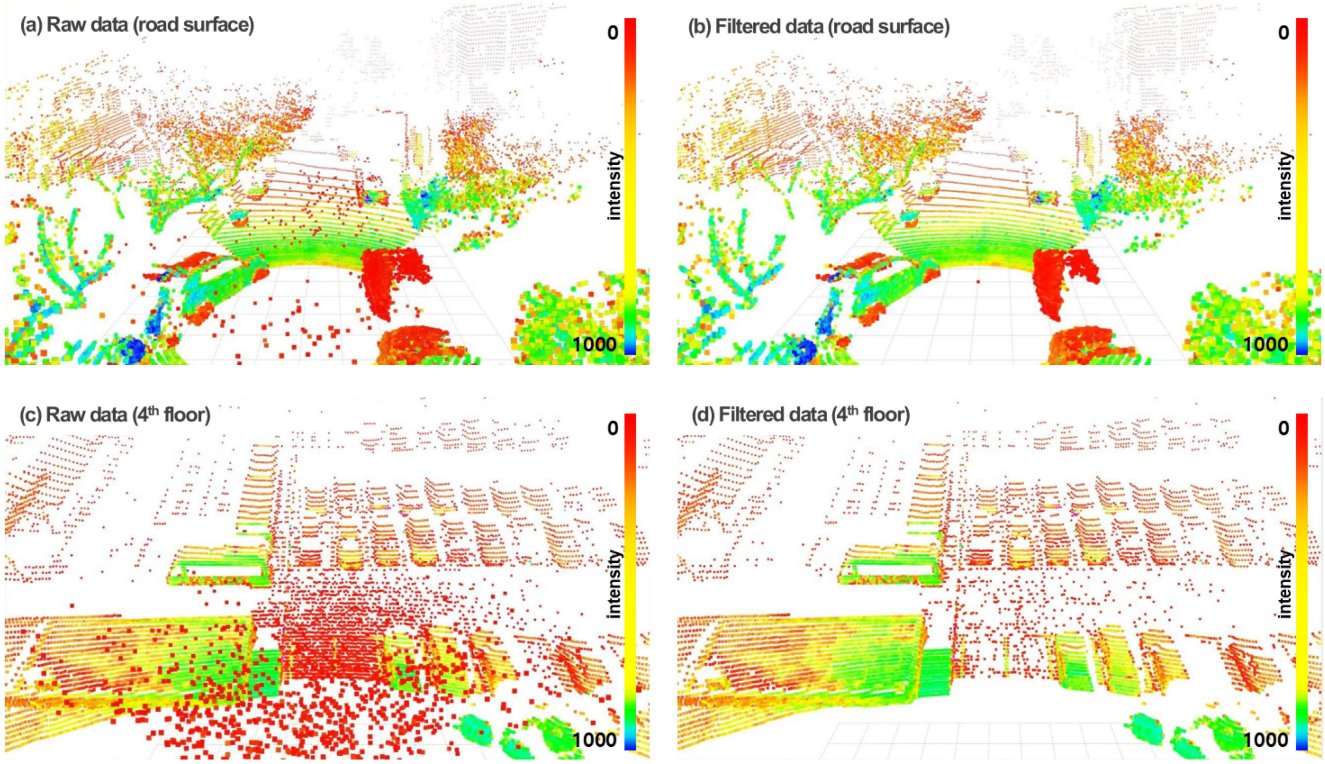


**FIGURE 10.** Comparison before and after applying the LIOR filter.

### C. DETERMINING THE SNOW DETECTION RANGE

Finally, in pseudocode line 3 in Algorithm 1, there is the concept of snow range, which is the maximum distance at which the LiDAR can physically detect snow particles. Because this parameter is a distance applied in the LIOR filter that affects the filtering speed, it must be calculated accurately. The point at which the intensity value falls below 1 in the snow intensity threshold curve (red line) in Fig. 9 corresponds to the theoretical distance at which the LiDAR can theoretically detect snow particles. Here, the calculated snow detection range ($d_s$) is 71.235 m.

## V. PERFORMANCE OF LIOR

### A. EXPERIMENTAL DATA COLLECTION

Data collection was performed using Ouster OS-1 64ch LiDAR, and we used an Nvidia Jetson Xavier to obtain a point cloud dataset that included falling snow of various sizes and densities over a one-week period. Additionally, to create a situation that maximized the noise effect caused by snow, the experimental sites included not only road surfaces but also the roofs of buildings. As a result of applying a rotation rate, vertical resolution, and horizontal resolution of 10 Hz, 64 ch, and 1,024 pts, respectively, for the LiDAR setup, a total of 65,536 points were obtained per frame [18].

### B. IMPLEMENTATION AND RESULT

We assigned the LIOR filter parameter searching radius ($r_s$), threshold number of neighbors ($n_{thr}$), and snow detection range ($d_s$) values of 0.1 m, 3 pts, and 71.235 m, respectively. The results of applying the proposed LIOR filter are presented in Fig. 10. The two left-hand images are the raw point cloud images before filtering, while the right-hand images show the result after snow removal with the LIOR filter. As shown in Fig. 10a, red noise points on the road surface correspond to actual snow; most of the red points around the tree are leaves. After filtering, the snow particles have been completely removed, as shown in Fig. 10b; even the distant buildings are clearly visible.

To collect point cloud data that contain considerable snow noise, similar to extreme environments in heavy snow, we acquired data from the roof of a building. The raw point cloud is shown in Fig. 10c, where it can be seen that substantially more snow noise was detected than in Fig. 10a. As shown in Fig. 10c, many more snow particles were generated than in the data obtained from the road surface. However, the LIOR filter was able to completely remove this noise, as shown in Fig. 10d.

### C. COMPARISONS WITH EXISTING FILTERS

We selected the SOR and DROR filters as comparisons for the proposed LIOR filter based on the results analyzed in Section II. The parameters applied to each filter are summarized in Table 1, and the snow removal performance results of each filter are compared in Fig. 11.

Considering the raw point cloud in the plan view, the snow particles falling around the LiDAR, parked roadside vehicles, trees, and buildings are visible. Because the point color was set to differ with the intensity, the intensity clearly decreases as the distance increases. The reason for low-intensity points

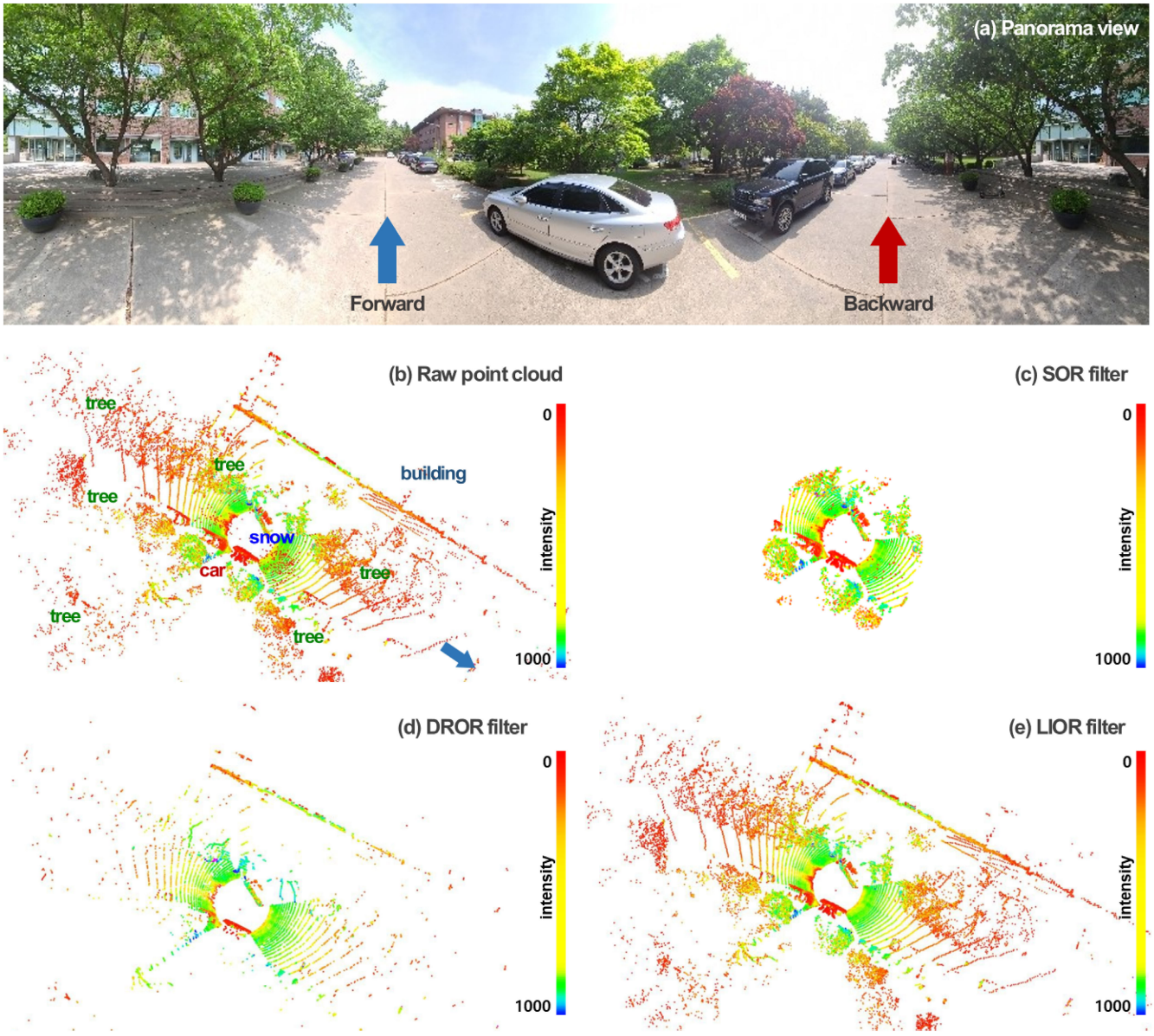


**FIGURE 11.** A comparison of the performance of SOR, DROR, and the proposed LIOR filter (Computing hardware: Intel Core i9-9900KF CPU @ 3.60GHz with 32 GB of RAM): (a) shows a panoramic view photo taken from the real LiDAR location to aid in understanding the point cloud image.

**TABLE 1.** Filter parameters.

| | Parameters | Value |
|---|---|---|
| SOR | number of neighbors | 3 |
| | standard deviation | 0.2 |
| DROR | searching radius | 0.1m |
| | min. number of neighbors | 3 |
| | radius multiplier | 3 |
| | azimuth angle | 0.16 |
| LIOR | searching radius | 0.1m |
| | min. number of neighbors | 3 |
| | snow detection range | 71.235m |
| | Intensity threshold constant | 0.066 |

even at short distances is because some objects have a low incident angle such as roads, vehicles with low reflectivity, and snow particles.

The SOR filter does not remove only the snow particles; it also removes all points above a certain distance from the LiDAR. This result occurs because, as explained as a disadvantage of the distance-based filter in Section II, as the distance from the LiDAR increases, the distance between the points becomes larger than the specified search radius; thus, all points located beyond a certain distance are removed as outliers. To remove snow particles, a smaller search radius can be applied, but then the circle shown in Fig. 11c decreases, causing most points to be lost. Similar results would be obtained if the ROR filter, another distance-based filter, were applied.

After applying the DROR filter, the snow particles were almost completely removed. However, the point clouds far from the LiDAR also suffer substantial losses even

though they contain important environmental information. The DROR results are a substantial improvement compared to the disadvantages of the distance-based ROR and SOR filters, but the DROR filter remains limited due to the losses in the surrounding point cloud data and because the filtering speed, which is a critical disadvantage of distance-based filters, has not been improved.

Meanwhile, the proposed LIOR filter not only completely removed snow particles but also showed excellent performance to perfectly preserve important environmental information without loss. In particular, it showed excellent performance of preserving even long-distance points with high probability of loss such as leaves of trees.

### D. EVALUATION

We evaluated the LIOR filter performance by comparing its speed and accuracy with the DROR filter.

#### 1) SPEED

First, Table 2 shows the filtering speed of each filter. The proposed LIOR filter is approximately 12 times faster than the SOR and 8 times faster than the DROR filter. However, this performance level can be used only in low-speed autonomous driving; it is unsuitable for high-speed autonomous driving applications. Therefore, to increase the performance of the LIOR filter to a level applicable in high-speed autonomous driving, the LIOR filter was applied only to the ROI (the road area ahead) to remove the need to process unnecessary data.

The actual size of the applied crop box is presented in Table 3 and visualized in Fig. 12. The reason for setting the x-axis direction to 119 m in the crop box size in Fig. 12b is that this value considers the minimum distance between the driver and the front bumper of the vehicle. Although the distance is only approximately 1 m, the point cloud in this area is the most densely formed; therefore, removing this section substantially improves the filtering speed. After applying the LIOR filter only to the ROI—the area in front and the road—the filtering speed improves, reaching up to 10 FPS, which is sufficient for use in actual high-speed autonomous driving.

Even though the ROI is reduced from the forward data to the road data, the filtering speed is improved only from 9.31 FPS to 10 FPS. This can be seen as a slight improvement in the filtering speed, but in practice, it means that the maximum speed cannot exceed 10 FPS because the rotation rate of the lidar sensor is 10 Hz. That is, since the frame rate of raw data is 10 FPS, the filtering rate cannot exceed 10 FPS. Therefore, when data are acquired at a speed exceeding 10 hz through advanced LiDAR in the future, the filtering speed of the LIOR filter will be much faster.

**TABLE 2.** Processing rate performance.

| | SOR | DROR | LIOR |
|---|---|---|---|
| Speed (FPS) | 0.11 | 0.16 | **1.32** |

**TABLE 3.** Optimizing the LIOR processing speed.

| | Size of cropbox (m) | Speed (FPS) |
|---|---|---|
| LIOR (Full data) | 240(x) × 240(y) × 49.7(z) | 1.32 |
| LIOR (Forward data) | 119(x) × 240(y) × 4.2(z) | 9.31 |
| LIOR (Road data) | 119(x) × 6(y) × 4.2(z) | **10.0** |

#### 2) ACCURACY

To evaluate the accuracy of the LIOR filter, we manually labeled the number of snow particles in 10 scans where the time stamps of the filtered images of the LIOR and DROR matched exactly. These hand-labeled data were then used to compare the performance of the DROR and LIOR filters. On average, each individual point cloud snapshot contained a total of 1098.8 snow particles. We evaluated the accuracy by comparing the number of points filtered by the DROR and LIOR filters based on these manually labeled snow points. The number of points filtered by each filter reached 32,097.7 for the DROR and 1,700.9 for the LIOR: the DROR filter removed approximately 18 times more points than the LIOR filter.

Fig. 13a shows the result of rendering the point filtered by the DROR and LIOR filters. The DROR filter deleted 48.9 % of the total point cloud data, which is nearly half the total point cloud data, which means that it does not distinguish between objects and environmental information well. In contrast, the LIOR filter removed 2.59 % of the points, a number similar to the labeled snow points. Additionally, unlike the DROR filter, the LIOR filter showed high accuracy in removing all snow points from the snow area, missing only eight points. The average percentage of filtered points per range is displayed in Fig. 13b. This result shows that the LIOR filter removes snow particles almost perfectly while minimizing the loss of environmental information.

To make the comparison easier to understand, we adopted three metrics to compare the filtering accuracy. The first metric is the *true positive rate*, which simply means the ratio of the number of filtered snow points in the areas where snow points can effectively be detected by LiDAR (the snow areas) to the number of manually labeled snow points in those areas. The second metric is the *false positive rate*, which is the ratio

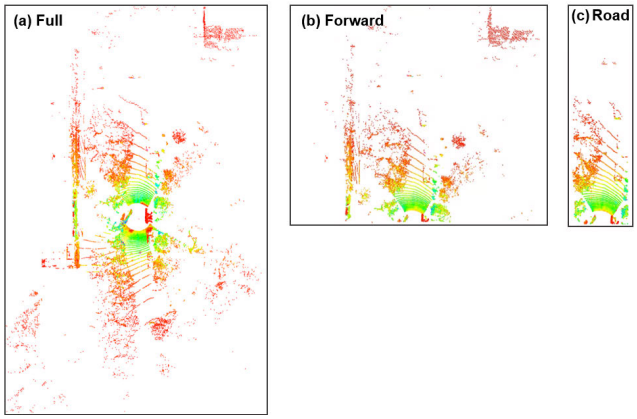


**FIGURE 12.** Size of the cropped point cloud.

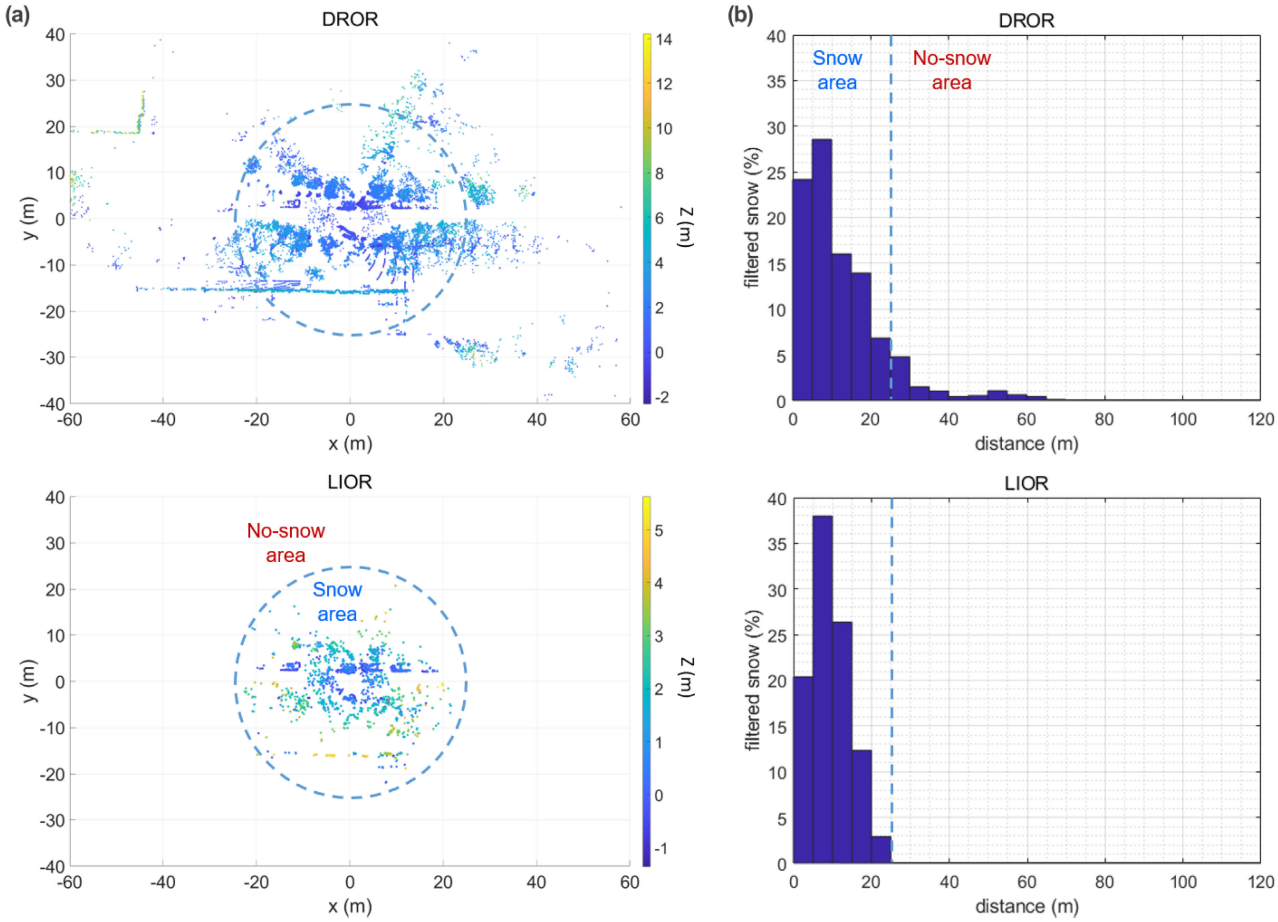


**FIGURE 13.** The average percentage of filtered points per range (a) and the rendered 3D image of the removed points (b).

of the number of filtered snow points in areas where snow particles cannot be sensed by LiDAR (the no-snow areas) compared to the number of manually labeled non-snow points in those areas. The last metric, *false negative rate*, is the ratio of the number of unfiltered snow points in the snow areas to the number of manually labeled snow points in those areas. The *true positive rate*, *false positive rate* and *false negative rate* are calculated by Equations (4), (5) and (6), respectively. The snow area and no-snow area can be understood more clearly through Fig. 13.

$$\text{True positive rate} = \frac{\text{filtered snow points in snow areas}}{\text{total labeled snow points}} \tag{4}$$

$$\text{False positive rate} = \frac{\text{filtered snow points in no-snow areas}}{\text{total labeled non-snow points}} \tag{5}$$

$$\text{False negative rate} = \frac{\text{unfiltered snow points in snow areas}}{\text{total labeled snow points}} \tag{6}$$

The areas where no snow particles exist on the point cloud can be estimated by calculating the distance to the farthest point among the hand-labeled snow points, which is 24.5 m.

**TABLE 4.** Filtering rate comparison: True positive rate closer to 100 %, false positive and false negative rates closer to 0 % indicate better performance.

| | DROR | LIOR |
|---|---|---|
| True positive rate (%) | $\approx 100$ | $\approx 100$ |
| False positive rate (%) | 48.11 | 0.93 |
| False negative rate (%) | $\approx 0$ | $\approx 0$ |

This result means that all areas farther than 24.5 m from the LiDAR location are considered to be no-snow areas. As shown by the *true positive* and *false negative rates* in Table 4, in the snow area, the DROR and LIOR filters almost completely removed the labeled snow points. However, as seen from the *false positive rate*, the DROR filter has a high rate of removing object points other than snow points, while the LIOR filter has a significantly lower value. This indicates that the LIOR filter does not remove important points that include environmental information; it mainly removes snow particles.

Thus far, to compare the performance of the LIOR and DROR filters, we have analyzed the accuracy with only 10 scans with matching time; however, to further verify the performance of the LIOR filter, a total of 50 additional scans were analyzed. The result of analyzing additional scans

confirmed the ability to completely remove snow particles, as expected, which is shown in Table 5. In addition to snowy weather, we tested the performance of LIOR filters in rainy weather, and the filtering results in Table 5 reveal that the rain removal performance is similar to the snow removal performance. In addition, as shown in Table 6, the filtering speed of rain demonstrated excellent performance, and when ROI was applied, as in the case of snow filtering, it had a fast filtering speed of up to 10 FPS. This confirmed that the LIOR filter perfectly removes not only snow points but also rain points at a very fast rate.

**TABLE 5. Verification of the performance accuracy of the LIOR filter with an additional dataset (50 scans without applying ROI).**

| | Snowy point cloud | Rainy point cloud |
|---|---|---|
| True positive rate (%) | $\approx 100$ | $\approx 100$ |
| False positive rate (%) | 0.85 | 0.68 |
| False negative rate (%) | $\approx 0$ | $\approx 0$ |

**TABLE 6. LIOR processing speed for a rainy point cloud.**

| | Size of cropbox (m) | Speed (FPS) |
|---|---|---|
| LIOR (Full data) | 240(x) × 240(y) × 49.7(z) | 1.78 |
| LIOR (Forward data) | 119(x) × 240(y) × 4.2(z) | 8.34 |
| LIOR (Road data) | 119(x) × 6(y) × 4.2(z) | **10.0** |

## VI. CONCLUSION

The proposed LIOR filter removes snow particles based on the intensity differences between snow particles and objects. When using this approach, the filtering speed and accuracy are noticeably improved compared to the existing filters. In particular, because the LIOR filter was designed to assume the maximum snow particle size, it is possible to perfectly filter any snow of any size. Moreover, point clouds collected by LiDAR in rainy weather conditions can be perfectly filtered. In this sense, this article is important because the proposed approach overcomes the disadvantage of LiDAR—its suceptibility to environmental changes—while maximizing the advantages of existing LiDAR sensors.

Although LiDAR sensors have substantial advantages over radar and optical cameras, many researchers assume that LiDAR sensor data should be excluded from ultimate autonomous driving implementations due to its weak ability to function under environmental noise conditions (e.g., rain, snow, fog). However, because this study resolves this drawback, it can be expected that the utilization of the LiDAR sensor will increase in the future. Moreover, as the resolution of LiDAR sensors is gradually improved to match that of image sensors, it is likely that this tendency will gradually accelerate. Future work includes verifying the object detection performance of LiDAR through filtered point clouds and applying the results to real-time autonomous vehicles.

## REFERENCES

[1] S. Ronnback and A. Wernersson, "On filtering of laser range data in snowfall," in *Proc. 4th Int. IEEE Conf. Intell. Syst.*, Sep. 2008, pp. 17–33, doi: 10.1109/IS.2008.4670551.

[2] R. H. Rasshofer, M. Spies, and H. Spies, "Influences of weather phenomena on automotive laser radar systems," *Adv. Radio Sci., ARS*, vol. 9, p. 49, Jan. 2011. [Online]. Available: https://search.proquest.com/docview/881207442?accountid=27828

[3] A. Filgueira, H. González-Jorge, S. Lagüela, L. Díaz-Vilariño, and P. Arias, "Quantifying the influence of rain in LiDAR performance," *Measurement*, vol. 95, pp. 143–148, Jan. 2017, doi: 10.1016/j.measurement.2016.10.009.

[4] R. Heinzler, P. Schindler, J. Seekircher, W. Ritter, and W. Stork, "Weather influence and classification with automotive lidar sensors," in *Proc. IEEE Intell. Vehicles Symp. (IV)*, Jun. 2019, pp. 1527–1534, doi: 10.1109/IVS.2019.8814205.

[5] M. Bijelic, T. Gruber, and W. Ritter, "A benchmark for lidar sensors in fog: Is detection breaking down?" in *Proc. IEEE Intell. Vehicles Symp. (IV)*, Jun. 2018, pp. 760–767, doi: 10.1109/IVS.2018.8500543.

[6] M. Kutila, P. Pyykonen, H. Holzhuter, M. Colomb, and P. Duthon, "Automotive LiDAR performance verification in fog and rain," in *Proc. 21st Int. Conf. Intell. Transp. Syst. (ITSC)*, Nov. 2018, pp. 1695–1701, doi: 10.1109/ITSC.2018.8569624.

[7] R. Heinzler, F. Piewak, P. Schindler, and W. Stork, "CNN-based lidar point cloud de-noising in adverse weather," *IEEE Robot. Autom. Lett.*, vol. 5, no. 2, pp. 2514–2521, Apr. 2020, doi: 10.1109/LRA.2020.2972865.

[8] H. Balta, J. Velagic, W. Bosschaerts, G. De Cubber, and B. Siciliano, "Fast statistical outlier removal based method for large 3D point clouds of outdoor environments," *IFAC-PapersOnLine*, vol. 51, no. 22, pp. 348–353, 2018, doi: 10.1016/j.ifacol.2018.11.566.

[9] N. Charron, S. Phillips, and S. L. Waslander, "De-noising of lidar point clouds corrupted by snowfall," in *Proc. 15th Conf. Comput. Robot Vis. (CRV)*, May 2018, pp. 254–261, doi: 10.1109/CRV.2018.00043.

[10] *Point Cloud Library Documentation*. Accessed: May 25, 2020. [Online]. Available: http://pointclouds.org/documentation/

[11] R. B. Rusu and S. Cousins, "3D is here: Point cloud library (PCL)," in *Proc. IEEE Int. Conf. Robot. Autom.*, May 2011, pp. 1–4, doi: 10.1109/ICRA.2011.5980567.

[12] X.-F. Han, J. S. Jin, M.-J. Wang, W. Jiang, L. Gao, and L. Xiao, "A review of algorithms for filtering the 3D point cloud," *Signal Process., Image Commun.*, vol. 57, pp. 103–112, Sep. 2017, doi: 10.1016/j.image.2017.05.009.

[13] L. Hui, L. Di, H. Xianfeng, and L. Deren, "Laser intensity used in classification of lidar point cloud data," in *Proc. IEEE Int. Geosci. Remote Sens. Symp. IGARSS*, 2008, doi: 10.1109/IGARSS.2008.4779201.

[14] S. P. Levashev, "Segmentation of a point cloud by data on laser scanning intensities," *Pattern Recognit. Image Anal.*, vol. 29, no. 1, pp. 144–155, Jan. 2019, doi: 10.1134/S1054661819010152.

[15] A. Kashani, M. Olsen, C. Parrish, and N. Wilson, "A review of LIDAR radiometric processing: From ad hoc intensity correction to rigorous radiometric calibration," *Sensors*, vol. 15, no. 11, pp. 28099–28128, Nov. 2015.

[16] A. Tatoglu and K. Pochiraju, "Point cloud segmentation with LIDAR reflection intensity behavior," in *Proc. IEEE Int. Conf. Robot. Autom.*, May 2012, pp. 786–790, doi: 10.1109/ICRA.2012.6225224.

[17] M. Cooper, J. Raquet, and R. Patton, "Range information characterization of the hokuyo UST-20LX LIDAR sensor," *Photonics*, vol. 5, no. 2, p. 12, May 2018, doi: 10.3390/photonics5020012.

[18] *Ouster OS1-LiDAR-Sensor-Datasheet.Pdf*, Ouster, San Francisco, CA, USA, 2020.

[19] J. Key, D. Santek, and R. Dworak, "Polar winds from shortwave infrared cloud tracking," in *Proc. 13th Int. Winds Workshop*, Jul. 2016, pp. 1–6.

[20] S.-H. Kim, D.-H. Ko, D.-K. Seong, S.-H. Eun, B.-G. Kim, B.-J. Kim, and J.-W. Cha, "Quantitative analysis of snow particles using a multi-angle snowflake camera in the Yeongdong region," *Atmosphere*, vol. 29, no. 3, pp. 311–324, Sep. 2019, doi: 10.14191/ATMOS.2019.29.3.311.

[21] J. Behley, V. Steinhage, and A. B. Cremers, "Efficient radius neighbor search in three-dimensional point clouds," in *Proc. IEEE Int. Conf. Robot. Autom. (ICRA)*, May 2015, pp. 3625–3630, doi: 10.1109/ICRA.2015.7139702.

[22] M. Muja and D. G. Lowe, "Fast approximate nearest neighbors with automatic algorithm configuration," in *Proc. VISAPP*, vol. 1, 2009, pp. 331–340, doi: 10.5220/0001787803310340.

**JI-IL PARK** (Student Member, IEEE) received the B.S. degree in mechanical engineering from the Korea Military Academy (KMA), Seoul, South Korea, in 2005, and the M.E. degree in mechanical engineering from the Korea Advanced Institute of Science and Technology (KAIST), Daejeon, South Korea, in 2013, where he is currently pursuing the Ph.D. degree in mechanical engineering. He was an Assistant Professor with the Department of Mechanical Engineering, Korea Military Academy (KMA), until 2019. His main research interests include LiDAR, radar, computer vision, and sensor fusion for self-driving vehicles.

**JIHYUK PARK** (Member, IEEE) received the B.S. and Ph.D. degrees in mechanical engineering from KAIST, Daejeon, South Korea, in 2011 and 2018, respectively. He was a Staff Engineer with the Mechatronics Research and Development Center, SAMSUNG Electronics Company. He is currently an Assistant Professor with the Department of Automotive Engineering, Yeungnam University. His research interests include mechatronic systems and robotic systems control, vibration control, autonomous driving, machine learning in robotics, and indoor/outdoor mobile robot navigation.

**KYUNG-SOO KIM** (Member, IEEE) received the B.S., M.S., and Ph.D. degrees in mechanical engineering from KAIST, Daejeon, South Korea, in 1993, 1995, and 1999, respectively. He has worked as the Chief Researcher of LG Electronics, Inc., from 1999 to 2003, and a DVD Front-End Manager with STMicroelectronics Company Ltd., from 2003 to 2005. In 2005, he joined the Department of Mechanical Engineering, Korea Polytechnic University, Gyeonggi, South Korea, as an Assistant Professor. Since 2007, he has been a Professor with the Department of Mechanical Engineering, KAIST, where he is currently the Head of the CCS Graduate School of Green Transportation. His research interests include digital system design for controlled mechatronics, actuator design, and control theory, such as robust controls and sliding mode controls.